Triple-point-type morphotropic phase boundary based large piezoelectric Pb-free material—$Ba(Ti_{0.8}Hf_{0.2})O_3$-$(Ba_{0.7}Ca_{0.3})TiO_3$

Chao Zhou,[1,2,a)] Wenfeng Liu,[2] Dezhen Xue,[1,3] Xiaobing Ren,[1,3] Huixin Bao,[1,4] Jinghui Gao,[1,2,3] and Lixue Zhang[4,5,a)]
[1]*Multi-disciplinary Materials Research Center, Frontier Institute of Science and Technology, Xi'an Jiaotong University, Xi'an 710054, China*
[2]*State Key Laboratory of Electrical Insulation and Power Equipment, School of Electrical Engineering, Xi'an Jiaotong University, Xi'an 710049, China*
[3]*Ferroic Physics Group, National Institute for Materials Science, 1-2-1 Sengen, Tsukuba 305-0047, Ibaraki, Japan*
[4]*State Key Laboratory for Mechanical Behavior of Materials, Xi'an Jiaotong University, Xi'an 710049, China*
[5]*International Center for Actuators and Transducers, Materials Research Institute, University Park, Pennsylvania 16802, USA*

(Received 14 March 2012; accepted 16 May 2012; published online 1 June 2012)

We report a large piezoelectric Pb-free system—$Ba(Ti_{0.8}Hf_{0.2})O_3$-$(Ba_{0.7}Ca_{0.3})TiO_3$, designed upon a triple-point morphotropic phase boundary (TMPB) idea. The system shows anomalies of both *ac* (dielectric and piezoelectric) and *dc* (P-E hysteresis) properties around TMPB, especially the d_{33} achieving ~550 pC/N at room temperature. Moreover, the detected *non-zero* thermal hysteresis around triple point shows a first order transition nature and non-isotropic polarization state, as well as verified by our theoretical Landau-type deduction, thus being considered as an important factor to influence the piezoelectricity along TMPB. Our work may stimulate the study on triple-point-related critical phenomena in other ferroic systems. © *2012 American Institute of Physics*. [http://dx.doi.org/10.1063/1.4724216]

Piezoelectricity refers to the coupling effect of a piezoelectric material between mechanical energy and electrical energy, which yields a mechanical-stress-induced polarization or an electrical-field-induced strain.[1,2] Such a capability of energy conversion makes piezoelectrics widely used in the devices which are requested to sense or generate electrical or strain signals, e.g., sensors, actuators, and transducers, etc.[1,2]

For more than half a century, Pb-based piezoelectrics (e.g., PZT, PMN-PT, and PZN-PT) have dominated the area of sensor and transducer technology. However, with the rising limitation of toxic lead, Pb-based materials are urgently facing a situation of being replaced.[3–7] Although intensive work has contributed to lead substitutes, quite few of the reported Pb-free materials can actually compete with PZT system.[6] This stimulates a lot of studies on the origin of high piezoelectricity in Pb-based materials and the exploration of Pb substitutes following the way of lead-containing piezoelectrics. It has been well recognized that the high piezoelectricity in Pb-based piezoelectrics is directly related to a morphotropic phase boundary (MPB) in the phase diagram[8] since the peak value like dielectric permittivity and piezoelectric coefficient (first derivative of polarization with respect to external *ac* field (stress or electric field)) naturally comes from the phase instability at phase transition point and thus can result in high performance. Besides, unlike that in a paraelectric-ferroelectric transition, which is not utilizable since the ferroelectrics will be depolarized once the temperature rises above Curie temperature (Tc), and unlike that in a normal ferroelectric-ferroelectric transition, which is also of little practical interest since its greatly limited value caused by a large energy barrier between the two ferroelectric phases (such as the case of tetragonal-orthorhombic transition of $BaTiO_3$), a MPB phase boundary deriving from triple point morphotropic phase boundary (TMPB) inherits the low energy barrier of triple point (TP)[9,10] between two ferroelectric phases involved in the transition and is generally treated as a phase boundary with *polarization isotropy*.[10–13] It thus contributes to the high performance of dominant lead-contained materials (also good temperature-independent stability with a vertical line) and also the recently reported lead-free materials, BCT-BZT (Refs. 11, 14–16) and BCT-BTS,[17] as shown in Figs. 1(a)–1(c).

Here in this work, based on the triple point MPB idea (and to distinguish it from other MPB lead-free materials without triple point) that is initially extracted from Pb-based piezoelectrics,[8,18,19] we designed a lead-free piezoelectric system, $(1\text{-}x)Ba(Ti_{0.8}Hf_{0.2})O_3$-$x(Ba_{0.7}Ca_{0.3})TiO_3$, which shows obvious anomalies (enhancement or suppression) of ferroelectric/piezoelectric/dielectric properties as approaching to the TMPB, especially the d_{33} reaching ~550 pC/N at room temperature, exceeding most of the current Pb-free piezoelectrics (d_{33} of high-end PZT is 590 pC/N).[4] Besides, experimentally detected non-zero thermal hysteresis around triple point, as well as theoretically verified by Landau-type deduction, indicates the important factors of polarization anisotropy at TP that inevitably influence the piezoelectric behavior along TMPB line, which need to be considered when designing similar systems.

The samples of $(1\text{-}x)Ba(Ti_{0.8}Hf_{0.2})O_3$-$x(Ba_{0.7}Ca_{0.3})TiO_3$ (denoted as BHT-*x*BCT hereinafter; *x* represents the mole fraction of $(Ba_{0.7}Ca_{0.3})TiO_3$) were fabricated with the conventional solid-state reaction method, with starting

a)Authors to whom correspondence should be addressed. Electronic addresses: zhouch1982@gmail.com and lixuezhang@gmail.com.

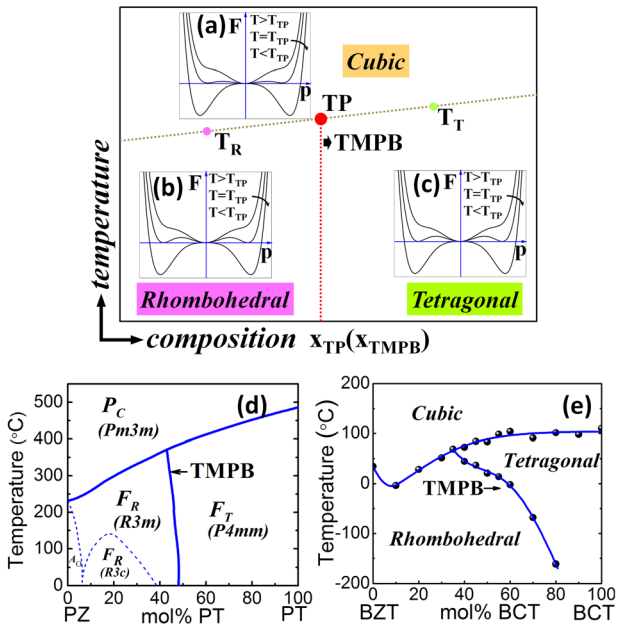

FIG. 1. A TMPB involved with two terminal compositions, which possess a common cubic parent phase, and two different ferroelectric phases—rhombohedral ferroelectric phase (R) and tetragonal ferroelectric phase (T). A TP appears at the intersection of two phase-boundary lines—Curie line and TMPB line. (a) Illustrates the Landau free energy profile with the temperature across TP for composition x_{TP}, and (b) and (c) illustrate the Landau free energy profiles with temperature across Curie line for compositions approaching to R and T terminals, with T_R and T_T represent the two paraelectric-ferroelectric transition temperatures, respectively. Phase diagram of binary piezoelectric $Pb(Zr_{1-x}Ti_x)O_3$ (d), and phase diagram of pseudo-binary $(1-x)Ba(Zr_{0.2}Ti_{0.8})O_3$-$x(Ba_{0.7}Ca_{0.3})TiO_3$ system (e).

chemicals of $CaCO_3$ (99.9%), $BaCO_3$ (99.95%), HfO_2 (98%), and TiO_2 (99.9%). The calcining was performed at 1350 °C in air for 2 h, and the sintering was performed at 1450 °C in air for 3 h.

For each composition, three forms of samples were prepared corresponding to different measurements: (1) The samples for measurements of dielectric and ferroelectric (*Polarization-Electric field* hysteresis loops) properties are in the form of sintered cylindrical pellets (unpoled), with a diameter of 7 mm and thickness of 1 mm, and were coated with silver paste as electrodes. The spectrum of dielectric permittivity was tested by a HIOKI3532 LCR meter at 100 Hz in a Delta temperature chamber. Ferroelectric properties (Polarization-Electric field loops) were measured with a ferroelectric tester (Radiant Workstation) at frequency of 10 Hz at room temperature (RT, 22 °C). (2) The samples for x-ray diffraction (XRD) test are in the form of sintered cylindrical pellets (unpoled), with a diameter of 7 mm and thickness of 1 mm. XRD test was carried out by the x-ray diffractometer Shimadzu XRD-7000. (3) The samples for test of piezoelectric coefficient d_{33} are cylinders with a diameter of 7 mm and thickness of 6 mm. Before piezoelectric measurements, the samples were poled at 22 °C for 1 h with an electric field of 1.2 kV/mm, and d_{33} was measured with a commercial Berlincourt-type d_{33} meter (ZJ-3A) for the poled samples.

The temperature spectrum of dielectric permittivity (Figs. 2(a1)–2(a4) show selected typical ones of BHT-0.1BCT, BHT-0.3BCT, BHT-0.5BCT, and BHT-0.7BCT) and the corresponding *in situ* XRD profiles (as shown in Figs. 2(b1)–2(b6), for a typical composition, BHT-0.5BCT) together construct the TMPB type phase diagram for pseudo-binary BHT-*x*BCT system (Fig. 2(c)). It can be seen that the two terminals, $Ba(Ti_{0.8}Hf_{0.2})O_3$ and $(Ba_{0.7}Ca_{0.3})TiO_3$, share a common parent phase above Curie temperature (Tc), and each undergoes only one phase transition [cubic (***C***) to rhombohedral (***R***) and cubic (***C***) to tetragonal (***T***), respectively] from 150 °C to −100 °C. And, the converging of three phases produces a triple point around BHT-0.3BCT (composition) and 55 °C (temperature).

It should be paid attention to that the peak value of permittivity spectrum of BHT-0.3BCT shows the highest value among those of all the samples is not a coincidence. This result indirectly suggests its weakest 1st order transition (close to 2nd order transition) within all the BHT-*x*BCT composition in the phase diagram we studied, which agrees well to the lowest anisotropy state at TP (BHT-0.3BCT is the composition closest to x_{TP} among all samples).

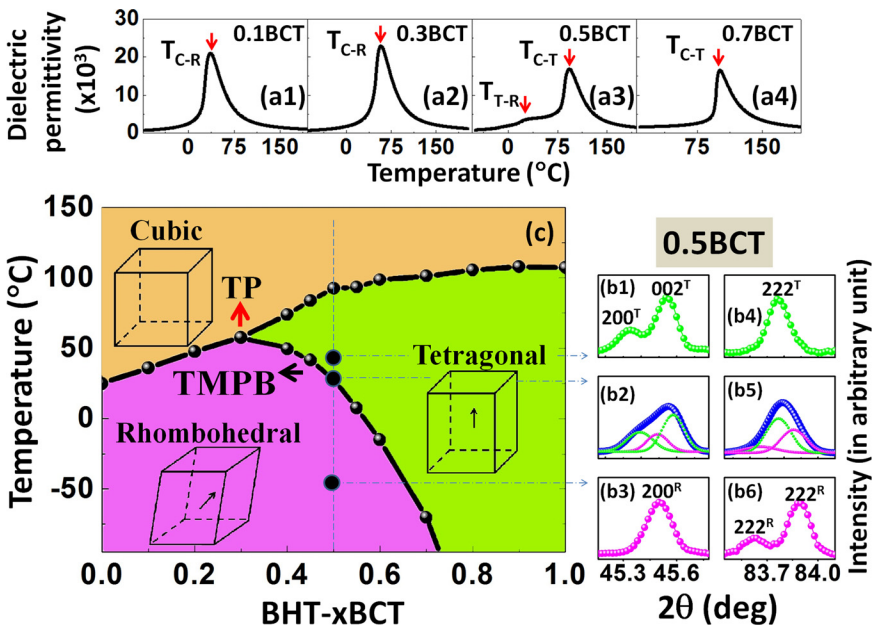

FIG. 2. Dielectric permittivity of BHT-0.1BCT (a1), BHT-0.3BCT (a2), BHT-0.5BCT (a3), BHT-0.7BCT (a4); x ray diffraction profiles of BHT-0.5BCT of (200) peak at 40 °C (b1), 22 °C (b2), −50 °C (b3), and of (222) peak at 40 °C (b4), 22 °C (b5), −50 °C (b6); phase diagram of pseudo-binary BHT-*x*BCT system (c).

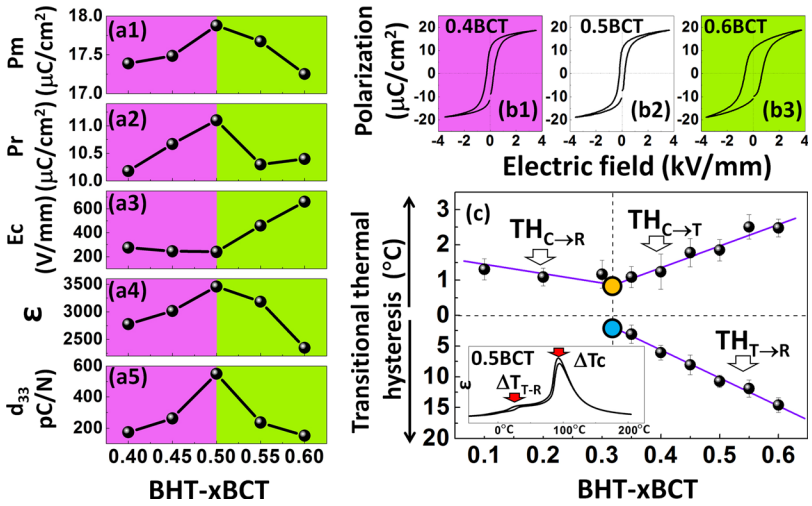

FIG. 3. Ferroelectric and piezoelectric properties of BHT-*x*BCT system with respect to composition around TMPB ($x = 0.5$, temperature ~22 °C), maximum polarization *Pm* (a1), remnant polarization *Pr* (a2), coercive field *Ec* (a3), dielectric permittivity ε (a4), piezoelectric coefficient d_{33} (a5); P-E hysteresis loops of BHT-0.4BCT (b1), BHT-0.5BCT (b2), BHT-0.6BCT (b3); transition thermal hysteresis for BHT-*x*BCT (*x*: 0.1-0.6) (c), with $TH_{C\to R}$, $TH_{C\to T}$, and $TH_{R\to T}$, representing the transition thermal hysteresis between different phases—cubic to rhombohedral, cubic to tetragonal, and rhombohedral to tetragonal, respectively.

Another inneglectable fact is that a consensus about the structure around TMPB has not been achieved.[10,11,20–25] For BHT-*x*BCT system, according to the phase diagram, the TMPB composition at RT is BHT-0.5BCT. The *in situ* x-ray diffraction profiles shown in Figs. 2(b1)–2(b3) reveal the evolution of characteristic peak 200 of BHT-0.5BCT at 40, 22, and −50 °C. And Figs. 2(b4)–2(b6) reveal the evolution of characteristic peaks 222 of BHT-0.5BCT at 40, 22, and −50 °C. Both groups of profiles show clearly BHT-0.5BCT undergoes a transition from T state (40 °C) to R state (−50 °C), with the intermediate state around TMPB (22 °C) corresponding to a superposition of T and R structures, revealing the coexistence of T and R phases around TMPB. The coexistence of R and T by TEM has also been verified in another Pb-free MPB system.[14] A detailed microscopic analyses on the structure of TMPB still are necessary.

Figs. 3(a1)–3(a5) and 3(b1)–3(b3) show the composition dependence (x = 0.40, 0.45, 0.50, 0.55, 0.60) of typical ferroelectric, dielectric and piezoelectric properties of BHT-*x*BCT at RT (22 °C). Figs. 3(a1)–3(a5) clearly reveal anomalies of properties appearing at BHT-0.5BCT (TMPB composition at RT)—the highest maximum polarization Pm (Fig. 3(a1)), the highest remnant polarization Pr (Fig. 3(a2)), the lowest coercive field Ec (Fig. 3(a3)), the highest dielectric permittivity ε (Fig. 3(a4)), and the highest piezoelectric coefficient d_{33} (Fig. 3(a5)). It should be emphasized that, the d_{33} of BHT-0.5BCT at room temperature (550 pC/N as shown in Fig. 3(a5)) is comparable to that of PZT-5H (~590 pC/N). Compared with TMPB composition sample BHT-0.5BCT, off-TMPB compositions exhibit much lower properties.

Fig. 3(c) shows the thermal hysteresis for the transitions of BHT-*x*BCT as a function of composition *x*. With *x* approaching to x_{TP} from both two terminal compositions, there is a monotonous decrease in the thermal hysteresis (between C and R, C and T, T and R), again suggesting the decrease of energy barrier between different states, thus contributing to the high performance at TMPB. The decrease of hysteresis also means that the 1st order nature of transition becomes weaker and weaker while *x* moves towards x_{TP}. Furthermore, minimization of polarization anisotropy corresponds to minimization of domain wall energy, which leads to miniaturization of domain structure.[23,26] Thus the appearance of nano-scaled domain configuration can be predicted. Actually the phenomenon has been observed in the famous TMPB-containing system, PZT.[24,27] And our group also observed similar nano-scaled domain configuration in Pb-free TMPB system.[14]

The above experimental results reveal that, all the property anomalies appearing at TMPB indicate the instability of response of polarization under external field, are caused by the weakening of polarization anisotropy around TMPB, well consisting with the theoretical analyses from the Landau type theoretical deduction.[9,15]

However, around TP, the carefully detected thermal hysteresis ~1 °C indicates the 1st order nature of transition, suggesting the assumption of polarization isotropy at MPB (the basic assumption of much MPB-related work) does not stand.[10–13,17] Here by a careful theoretical analysis, we will show that polarization is not necessarily isotropic at TP, and high performance is directly related with low energy barrier of TMPB itself, while the polarization anisotropy at TP will affect the properties along TMPB line, which need to be considered when designing similar systems.

To analyze the relationship between high properties and TMPB phase boundary, we employ a simple Landau-type model. The expression of free energy for ferroelectrics can be written in terms of polarization components, (P_1, P_2, P_3)[28,29]

$$\begin{aligned} F = F_0 + \Delta F &= F_0 + \alpha_{(x,T)}P_0^2 + \beta_{1(x,T)}(P_1^4 + P_2^4 + P_3^4) \\ &+ \beta_{2(x,T)}(P_1^2P_2^2 + P_2^2P_3^2 + P_3^2P_1^2) + \gamma_{1(x,T)}(P_1^6 + P_2^6 + P_3^6) \\ &+ \gamma_{2(x,T)}[P_1^4(P_2^2 + P_3^2) + P_2^4(P_1^2 + P_3^2) + P_3^4(P_1^2 + P_2^2)] \\ &+ \gamma_{3(x,T)}P_1^2P_2^2P_3^2, \end{aligned} \quad (1)$$

where $\alpha_{(x,T)}$, $\beta_{1(x,T)}$, $\beta_{2(x,T)}$, $\beta_{3(x,T)}$, $\gamma_{1(x,T)}$, $\gamma_{2(x,T)}$, and $\gamma_{3(x,T)}$ are all temperature and composition dependent coefficients; P_0 is the absolute value of polarization which is defined by $P_0 = \sqrt{P_1^2 + P_2^2 + P_3^2}$.

At TP, the conditions for three phases (cubic parent phase, tetragonal ferroelectric phase, rhombohedral ferroelectric phase in the present designed phase diagram) coexisting in equilibrium give

$$\Delta F_R = \Delta F_T = \Delta F_C = 0, \tag{2}$$

$$\frac{\partial F_R}{\partial P_R} = \frac{\partial F_T}{\partial P_T} = 0, \tag{3}$$

$$\frac{\partial^2 F_R}{\partial P_R^2} \geq 0, \quad \frac{\partial^2 F_T}{\partial P_T^2} \geq 0. \tag{4}$$

Then the relation between coefficients is obtained

$$\beta_{2(x_{TP},T_C)} = 2\beta_{1(x_{TP},T_C)}, \tag{5a}$$

$$24\gamma_{1(x_{TP},T_C)} - 6\gamma_{2(x_{TP},T_C)} - \gamma_{3(x_{TP},T_C)} = 0. \tag{5b}$$

After substituting (5a) and (5b) into (1), the expression of free energy at TP turns to be

$$\begin{aligned} F = F_0 + \alpha_{(x_{TP},T_C)}P_0^2 + \beta_{1(x_{TP},T_C)}P_0^4 + \gamma_{1(x_{TP},T_C)}P_0^6 \\ + (\gamma_{2(x_{TP},T_C)} - 3\gamma_{1(x_{TP},T_C)})[P_1^4(P_2^2+P_3^2) + P_2^4(P_1^2+P_3^2) \\ + P_3^4(P_1^2+P_2^2)] + (\gamma_{3(x_{TP},T_C)} - 6\gamma_{1(x_{TP},T_C)})P_1^2P_2^2P_3^2. \end{aligned} \tag{6}$$

Equation (6) reveals that the 4th term of free energy is isotropic and the 6th term is not isotropic (the condition for 6th term being isotropic is $\gamma_{3(x_{TP},T_C)} = 2\gamma_{2(x_{TP},T_C)} = 6\gamma_{1(x_{TP},T_C)}$). Non-isotropicity (polarization-dependence of free energy) at TP naturally leads to an energy barrier between different stable phases limited by anisotropy, which induces a thermal hysteresis and defines a 1st order phase transition in nature (Fig. 1(a)). And the 1st order nature transition is deduced from a model with only polarization terms involved, not to mention the effect of strain-polarization coupling terms which are supposed to be considered in ferroic systems when the order of transition is investigated.[30] The deduction is well verified by the careful measurements in this work which detect the thermal hysteresis with composition x approaching to x_{TP} and the results proved its weak 1st order transition nature.

Near the Curie line, the convergence of the Landau series for second order and weak first order transitions suggests the contributions of 6th and higher-order anisotropy terms are quite small.[31] Here only the region near TP is discussed, so the contribution of anisotropy taken by 6th order term can be neglected and the 4th term plays the leading role. While composition x deviates x_{TP} (TP composition), $\beta_2 \neq 2\beta_1$ and anisotropy on Curie line increases, inducing an increased energy barrier between paraelectric phase and ferroelectric phase (Figs. 1(b) and 1(c)).[10]

Then we analyze whether the TMPB can induce high performance, taking dielectric permittivity as an example as its simple relation with electric field. The dielectric permittivity is given as

$$\varepsilon_{ij} = \frac{\partial P_i}{\partial E_j} = \frac{\partial P_i}{(\partial F/\partial P_j)} = 1 \Big/ \left(\frac{\partial^2 F}{\partial P_i \partial P_j}\right). \tag{7}$$

In tetragonal (**T**) phase, $\bar{P}_T = (P_1, P_2, P_3) = (0, 0, P_T)$ and permittivity is obtained as

$$\varepsilon_{11} = \frac{1}{2(\beta_{2(x,T)} - 2\beta_{1(x,T)})P_T^2 + 2(\gamma_{2(x,T)} - 3\gamma_{1(x,T)})P_T^4}. \tag{8}$$

ε_{22} and ε_{33} can also be calculated (in tetragonal phase)

$$\varepsilon_{22} = \varepsilon_{11} = \frac{1}{2(\beta_{2(x,T)} - 2\beta_{1(x,T)})P_T^2 + 2(\gamma_{2(x,T)} - 3\gamma_{1(x,T)})P_T^4}, \tag{9}$$

$$\varepsilon_{33} = \frac{1}{8\beta_{1(x,T)}P_T^2 + 24\gamma_{1(x,T)}P_T^4}. \tag{10}$$

For the ideal case—TMPB being vertical, which means x_{TMPB} (TMPB composition) equals x_{TP} and the phase transition (between two ferroelectric phases below Curie line) is not temperature-driven but composition-driven, indicating that the coefficients of 4th terms and 6th terms are all temperature-independent and composition-dependent. Thus when $x = x_{TMPB}$, ε_{11}, and ε_{22} achieve an ultrahigh maximum value, reflecting a transverse instability with respect to polarization.[13,32] And meanwhile, ε_{33} achieves a maximum value due to a longitudinal instability of polarization caused by the extension of polarization at phase transition. And both types of instability suggest that for a TMPB-based ceramic system, the dielectric permittivity at certain temperature reaches a maximum at x_{TMPB}. The results for rhombohedral (**R**) phase follow the similar way as above tetragonal phase.

As for piezoelectricity, it consists of two parts of contribution, one is from the degree of polarization anisotropy, and the other one is from the degree of lattice softening.[33] Since the low polarization anisotropy and elastic softening always go hand in hand,[33] the high piezoelectricity, accompanying the high dielectric permittivity at TMPB, is reasonably expected. Further work will focus on the detailed theoretical analyses of these complicated equations.

The theoretical deduction and its well verification by experimental results clearly indicates that high performance itself along TMPB is not necessarily related with the polarization isotropy at TP, while closely decided by the lower energy barrier inherits from the TP. Obviously, the BHT-xBCT system reported in this work possesses a phase diagram quite similar to that of PZT (Fig. 1(d))[8] and that of a recently discovered Pb-free system BZT-BCT (Fig. 1(e)).[11] Besides, other well-known Pb-based piezoelectrics, such as PMN-PT and PZN-PT,[34,35] all possess phase diagrams conforming to Fig. 1, except that their TMPB are not vertical but tilted in different levels. For the case of tilted TMPB, away from TP and along TMPB, energy barrier between different states increases. But since the TMPB is the phase boundary, the thermodynamic equilibrium conditions define it as the boundary with the lowest anisotropy isothermally. In other words, TMPB always characterizes the state with the lowest polarization anisotropy below the Curie line within the phase diagram, which facilitates the polarization rotation and domain movement, resulting in a high sensitivity to external field, as evidenced by the results in Figs. 3(a1)–3(a5). By appropriate choice of two terminals (with different phases at low temperature region, including ferroelectric, antiferroelectric, relaxor, etc.) constructing TMPB phase diagram, fabrication of high-performance piezoelectrics approaching PZT or better (with high Tc and weak temperature dependence) are quite probable.

It should be also stressed that the isotropic polarization is not necessary at TP as has been treated in previous work[10–12] which reported the tricriticality (crossover point from 1st order to 2nd order phase transition). However, the tricriticality in BCT-BZT indicates an even lower energy barrier along TMPB and thus reasonably higher property compared with current system BHT-BCT, although Hf was the most similar ions as Zr in the respect of influencing phase transition of matrix of BT. This thus suggests to be an important factor to be considered when designing enhanced property following TMPB idea. It is also noticed that, with approaching to Tc along TMPB line, the polarization anisotropy weakens, and the corresponding ac properties (piezoelectricity, dielectric permittivity) will be enhanced.[15] It thus becomes significant to well balance a high Tc and high piezoelectricity when constructing TMPB system.

In addition, except for the important role of triple point to the polarization rotation discussed here, a contribution from polarization extension can be smartly added through a non-polar end-member as mentioned in Ref. 32 in TMPB phase diagram. It will thus become an even powerful idea for searching high performance materials.

Last but not least, it should be noticed that TMPB-related phenomena exist not only in ferroelectrics. A recent study even reported TMPB-related anomalous properties in ferrimagnetic materials.[36] From the physical parallelism of different ferroic systems,[37] it is anticipated that TMPB-related phenomena exist in all ferroic systems or even beyond the domain of ferroics, as long as the material system adopts a phase boundary derived from TP (like TMPB), which yields the lowest anisotropy of order parameters (like polarization in ferroelectrics).

In conclusion, based on theoretical analysis of TMPB phase diagram, a Pb-free piezoelectric system, $Ba(Ti_{0.8}Hf_{0.2})O_3$-$(Ba_{0.7}Ca_{0.3})TiO_3$ was designed. The system exhibits expected anomalies of properties at TMPB and even shows a high $d_{33} \sim 550$ pC/N (comparable to that of high-end PZT) at RT. The attempt in this work indicates a generally effective TMPB approach (from the similarity between the phase diagram of BHT-xBCT system to those of other high performance systems, e.g. PZT, PMN-PT, BZT-BCT, BTS-BCT) to obtain high-performance piezoelectrics, especially Pb-free ones. Besides, it is confirmed from both theoretical and experimental views that high performance is closely related with low energy barrier of TMPB, while polarization isotropy at TMPB (or tricriticality of TP) actually is not necessary though it benefits even higher property. Our study may stimulate interests and careful system design towards TP-related critical phenomena in ferroic materials or even a wider range of material systems.

The authors are grateful to Yonggang Yao, Sen Yang, and Haijun Wu for helpful discussions. This work was supported by Kakenhi of JSPS (X. Ren), National Basic Research Program of China (Grant Nos. 2010CB631003 and 2012CB619401), the National Natural Science Foundation of China (Grant Nos. 51007070 and 51072158), the NCET and 111 project of China (Grant No. B06025), and State Key Laboratory of Electrical Insulation and Power Equipment, Xi'an Jiaotong University (EIPE10301).

[1]Morgan Matroc Ltd. Transducer Products Division, *Piezoelectric Ceramics Data Book for Designers* (2002).
[2]J. F. Tressler, S. Alkoy, and R. E. Newnham, J. Electroceram. **2**, 257 (1998).
[3]E. Cross, Nature (London) **432**, 24 (2004).
[4]Y. Saito, H. Takao, T. Tani, T. Nonoyama, K. Takatori, T. Homma, T. Nagaya, and M. Nakamura, Nature (London) **432**, 84 (2004).
[5]T. Takenaka and H. Nagata, J. Eur. Ceram. Soc. **25**, 2693 (2005).
[6]T. R. Shrout and S. J. Zhang, J. Electroceram. **19**, 113 (2007).
[7]P. K. Panda, J. Mater. Sci. **44**, 5049 (2009).
[8]B. Jaffe, W. R. Cook, and H. Jaffe, *Piezoelectric Ceramics* (Academic, New York, 1971).
[9]R. E. Cohen and H. X. Fu, Nature (London) **403**, 281 (2000).
[10]G. A. Rossetti, A. G. Khachaturyan, G. Akcay, and Y. Ni, J. Appl. Phys. **103**, 114113 (2008).
[11]W. F. Liu and X. B. Ren, Phys. Rev. Lett. **103**, 257602 (2009).
[12]M. Porta and T. Lookman, Phys. Rev. B **83**, 174108 (2011).
[13]Y. Ishibashi and M. Iwata, Jpn. J. Appl. Phys. 2 **37**, L985 (1998).
[14]J. H. Gao, D. Z. Xue, Y. Wang, D. Wang, L. X. Zhang, H. J. Wu, S. W. Guo, H. X. Bao, C. Zhou, W. F. Liu, S. Hou, G. Xiao, and X. B. Ren, Appl. Phys. Lett. **99**, 092901 (2011).
[15]H. X. Bao, C. Zhou, D. Z. Xue, J. H. Gao, and X. B. Ren, J. Phys. D: Appl. Phys. **43**, 465401 (2010).
[16]D. Z. Xue, Y. M. Zhou, H. X. Bao, C. Zhou, J. H. Gao, and X. B. Ren, J. Appl. Phys. **109**, 054110 (2011).
[17]D. Z. Xue, Y. M. Zhou, H. X. Bao, J. H. Gao, C. Zhou, and X. B. Ren, Appl. Phys. Lett. **99**, 122901 (2011).
[18]J. S. Forrester, R. O. Piltz, E. H. Kisi, and G. J. McIntyre, J. Phys. – Condens. Matter **13**, L825 (2001).
[19]B. Noheda, D. E. Cox, G. Shirane, J. Gao, and Z. G. Ye, Phys. Rev. B **66**, 054104 (2002).
[20]S. K. Mishra, A. P. Singh, and D. Pandey, Philos. Mag. B **76**, 213 (1997).
[21]B. Noheda, J. A. Gonzalo, L. E. Cross, R. Guo, S. E. Park, D. E. Cox, and G. Shirane, Phys. Rev. B **61**, 8687 (2000).
[22]B. Noheda, R. Guo, L. E. Cross, S. E. Park, D. E. Cox, and G. Shirane, Phys. Rev. Lett. **84**, 5423 (2000).
[23]G. A. Rossetti and A. G. Khachaturyan, Appl. Phys. Lett. **91**, 072909 (2007).
[24]K. A. Schonau, L. A. Schmitt, M. Knapp, H. Fuess, R.-A. Eichel, H. Kungl, and M. J. Hoffmann, Phys. Rev. B **75**, 184117 (2007).
[25]R. E. Cohen, M. Ahart, M. Somayazulu, P. Ganesh, P. Dera, H. K. Mao, R. J. Hemley, Y. Ren, P. Liermann, and Z. G. Wu, Nature (London) **451**, 545 (2008).
[26]M. E. Lines and A. M. Glass, *Principles and Applications of Ferroelectrics and Related Materials* (Clarendon, Oxford, 1977).
[27]L. A. Schmitt, K. A. Schonau, R. Theissmann, H. Fuess, H. Kungl, and M. J. Hoffmann, J. Appl. Phys. **101**, 074107 (2007).
[28]A. F. Devonshire, Philos. Mag. Ser. 7 **40**, 1040 (1949).
[29]A. F. Devonshire, Philos. Mag. Ser. 7 **42**, 1065 (1951).
[30]S. Yang, X. Ren, and X. Song, Phys. Rev. B **78**, 174427 (2008).
[31]B. A. Strukov and A. P. Levanyuk, *Ferroelectric Phenomena in Crystals* (Springer, Berlin, 1998).
[32]D. Damjanovic, Appl. Phys. Lett. **97**, 062906 (2010).
[33]M. Iwata, H. Orihara, and Y. Ishibashi, Ferroelectrics **266**, 57 (2002).
[34]J. Kuwata, K. Uchino, and S. Nomura, Ferroelectrics **37**, 579 (1981).
[35]S. W. Choi, T. R. Shrout, S. J. Jang, and A. S. Bhalla, Mater. Lett. **8**, 253 (1989).
[36]S. Yang, H. X. Bao, C. Zhou, Y. Wang, X. B. Ren, Y. Matsushita, Y. Katsuya, M. Tanaka, K. Kobayashi, X. P. Song, and J. R. Gao, Phys. Rev. Lett. **104**, 197201 (2010).
[37]V. K. Wadhawan, *Introduction to Ferroic Materials* (Gordon and Breach, Amsterdam, 2000).